AFGL-TR-88-0127
ENVIRONMENTAL RESEARCH PAPERS, NO. 1003

Cross Field Transport of Electrons: Implications for the POLAR Code, Spacecraft Charging

David L. Cooke
Charles Dubs
Michael Heinemann

17 May 1988

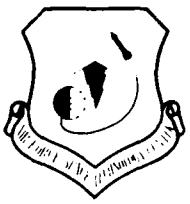

SPACE PHYSICS DIVISION PROJECT 7601
AIR FORCE GEOPHYSICS LABORATORY
HANSCOM AFB, MA 01731

"This technical report has been reviewed and is approved for publication"

FOR THE COMMANDER

CHARLES P. PIKE
Branch Chief

RITA C. SAGALYN
Director

This document has been reviewed by the ESD Public Affairs Office (PA) and is releasable to the National Technical Information Service (NTIS).

Qualified requestors may obtain additional copies from the Defense Technical Information Center. All others should apply to the National Technical Information Service.

If your address has changed, or if you wish to be removed from the mailing list, or if the addressee is no longer employed by your organization, please notify AFGL/DAA, Hanscom AFB, MA 01731. This will assist us in maintaining a current mailing list.

Do not return copies of this report unless contractual obligations or notices on a specific document requires that it be returned.

UNCLASSIFIED
SECURITY CLASSIFICATION OF THIS PAGE

ADA204392

REPORT DOCUMENTATION PAGE

1a. REPORT SECURITY CLASSIFICATION Unclassified	1b. RESTRICTIVE MARKINGS
2a. SECURITY CLASSIFICATION AUTHORITY	3. DISTRIBUTION / AVAILABILITY OF REPORT Approved for public release; distribution unlimited.
2b. DECLASSIFICATION / DOWNGRADING SCHEDULE	
4. PERFORMING ORGANIZATION REPORT NUMBER(S) AFGL-TR-88-0127 ERP, No. 1003	5. MONITORING ORGANIZATION REPORT NUMBER(S)
6a. NAME OF REPORTING ORGANIZATION Air Force Geophysics Laboratory 6b. OFFICE SYMBOL (If Applicable) PHK	7a. NAME OF MONITORING ORGANIZATION
6c. ADDRESS (City, State, and ZIP Code) Hanscom AFB Massachusetts 01731-5000	7b. ADDRESS (City, State, ZIP Code)
8a. NAME OF FUNDING / SPONSORING ORGANIZATION 8b. OFFICE SYMBOL (If Applicable)	9. PROCUREMENT INSTRUMENT IDENTIFICATION NUMBER
8c. ADDRESS (City, State, ZIP Code)	10. SOURCE OF FUNDING NUMBERS PROGRAM ELEMENT NO. 62101F; PROJECT NO. 7601; TASK NO. 30; WORK UNIT ACCESSION NO.

11. TITLE (Include Security Classification)
Cross Field Transport of Electrons: Implications for the POLAR Code, Spacecraft Charging

12. PERSONAL AUTHOR(S)
Cooke, D.L., Dubs, C., and Heinemann, M.

13. TYPE OF REPORT	13b. TIME COVERED	14. DATE OF REPORT (Year, Month, Day)	15. PAGE COUNT
Scientific Interim	FROM _____ TO _____	1988 May 17	22

16. SUPPLEMENTARY NOTATION

17. COSATI CODES		
FIELD	GROUP	SUB-GROUP

18. SUBJECT TERMS (Continue on reverse if necessary and identify by block number)
Cross field transport,
Electron collection,
Spacecraft charging, plasma sheaths.

19. ABSTRACT (Continue on reverse if necessary and identify by block number)

Early studies of electron transport in crossed E and B fields have been reviewed and applied to the case of a positive surface moving in the ionosphere. That work points to the importance of the parameter $q = \omega_{pi}^2 / \omega_{ce}^2$ in determining self-consistent spacecharge distributions in cross field diodes, and similarly, a crossed field probe-plasma sheath in non-liner, non-adiabatic limits. The application of existing theory to the problem of electron collection by a surface aligned with B indicates that for $q > 1/2$ the plasma sheath is only slightly perturbed by B, but for $q < 1/2$ the sheath cannot form without electrons transported along B from the ends.

20. DISTRIBUTION/AVAILABILITY OF ABSTRACT	21. ABSTRACT SECURITY CLASSIFICATION
☒ UNCLASSIFIED/UNLIMITED ☐ SAME AS RPT. ☐ DTIC USERS	Unclassified

22a. NAME OF RESPONSIBLE INDIVIDUAL	22b. TELEPHONE (Include Area Code)	22c. OFFICE SYMBOL
DAVID L. COOKE	(617) 377-2931	AFGL/PHK

DD FORM 1473, 84 MAR 83 APR edition may be used until exhausted. All other editions are obsolete.

SECURITY CLASSIFICATION OF THIS PAGE
UNCLASSIFIED

Contents

Illustrations

Cross Field Transport of Electrons: Implications for the POLAR Code, Spacecraft Charging

1. INTRODUCTION

The emission of a high power electron beam from a vehicle in space can lead to a positive spacecraft potential thousands of times greater than the ambient plasma temperature. A requirement of the POLAR code[1,2] is that it be able to model this interaction accurately in three dimensions, including the Earth's magnetic field. Recent work at AFGL has been aimed at validating POLAR in this limit by comparison with Magnetron Theory as a way of testing its electron tracking accuracy. POLAR predictions of electron collection in a magnetized plasma will ultimately have to match or be reconciled with the theories of Rubinstein and Laframboise[3] and Parker and Murphy[4]. These studies however, use either drift theory or orbit classification to avoid detailed trajectory tracking, thus not allowing the detailed evaluation of the POLAR method that we seek.

(Received for Publication 16 May 1988)

1. Cooke, D.L., Katz I., Mandell, M.J., Lilley, J.R., Jr., and Rubin, A.J. (1983) Three-dimensional calculation of shuttle charging in polar orbit, in proc. *Spacecraft Environmental Interactions Tech.* Conf. ed. by C.K. Purvis and C.P. Pike, NASA Conf. Pub. 2359, AFGL-TR-85-0018.
2. Lilley, J.R., Jr., Cooke, D.L., Jongward, G.A., and Katz, I. (1985) *Polar User's Manual*, AFGL-TR-85-0246, AD A173 758.
3. Rubinstein, J. and Laframboise, J.G. (1983) Theory of axially symetric probes in a collisionless magnetoplasma: aligned spheroids, finite cylinders, and disks, *Phys. Fluids* **26**:12.
4. Parker, L.W. and Murphy, B.L. (1967) Potential buildup on an electron-emitting ionospheric satellite, *J. Geophys. Res.* **72**:5.

The planar magnetron has been studied by many authors; Page and Adams[5], Birdsall and Bridges[6] both present analysis of greater detail than that provided here, which is only sufficient to properly identify the parameters that bear upon our application. Our approach is then to use a space charge limited diode model, with magnetic field, to characterize the sheath about a probe or spacecraft in the ionosphere.

2. THE B-SHEATH

The analysis that we present here is that of a steady state 'Magnetron' planar sheath with crossed electric E and magnetic fields B (Figure 1). It is not a complete magnetized-plasma-probe theory, but we feel that our 'B-Sheath' solution can provide insight similar to that provided by the Child-Langmuir[7,8] model for the non-magnetized sheath by identifying the key parameters and characteristics of the problem.

Figure 1 illustrates the situation where electrons are emitted from the sheath edge at z = 0, with density n_o, and velocity $\dot{z}_o$. We take the transverse velocity to be $\dot{x}_o = 0$ at the sheath edge, as well as the potential, V. The electron charge and mass are –e and m, **B** is in the $\hat{y}$ direction and **E** is in the $\hat{z}$ direction.

Our equations are thus:

Force,

$$m\ddot{x} = eB\dot{z} \tag{1}$$

$$m\ddot{z} = eE - eB\dot{x} \tag{2}$$

Energy,

$$\tfrac{1}{2}m(\dot{x}^2 + \dot{z}^2) - eV = \tfrac{1}{2}m\dot{z}_o^2 \tag{3}$$

The connection between a diode model and a plasma sheath is made by recognizing that the flux is provided by some net drift, v_d, so for continuity we have,

$$n(z)\dot{z}(z) = n_o v_d, \tag{4}$$

and Poisson's Equation,

$$d^2V/dz^2 = en(z)/\epsilon_o = en_o v_d/\epsilon_o\dot{z} = (en_o\dot{z}_o/\epsilon_o\dot{z})\, M_e \tag{5}$$

---

5. Page, L. and Adams, N.I., Jr. (1946) Space charge in plane magnetron, *Phys. Rev.* **69**:9, 10.
6. Birdsall, C.K. and Bridges, W.B. (1966) *Electron Dynamics of Diode Regions*, Academic Press Electrical Science Series.
7. Child, C.D. (1911) Discharge from hot CaO, *Phys. Rev.* Ser. I, **32**:492.
8. Langmuir, I. (1923) The effect of space charge and initial velocities on the potential distribution and thermionic current between plane parallel electrodes, *Phys. Rev.* **21**:419.

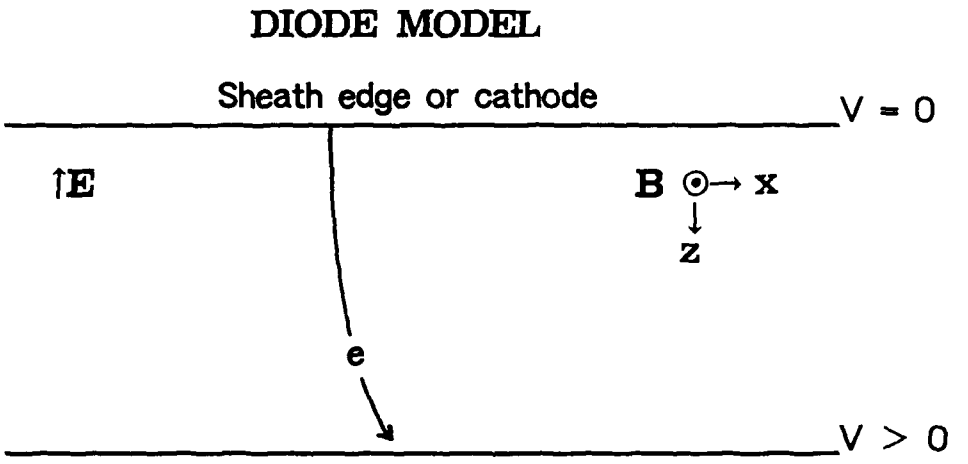

Figure 1. Diagram illustrating a crossed field diode or plasma sheath. The sheath edge is modeled as a cathode where both the electric field and potential are taken to be zero.

where Eq. (4) has been employed and we have defined $M_e = v_d/\dot{z}_o$ as the electron mach velocity by identifying $\dot{z}_o$ as the electron thermal speed.

Integrate Eq. (1), set $x_o = 0$, and substitute into Eq. (3) to get

$$\omega_c^2 z^2 + \dot{z}^2 - 2eV/m = \dot{z}_o^2 \tag{6}$$

where $\omega_c = eB/m$ is the electron cyclotron frequency. Differentiating twice by z (using $d/dz = \dot{z}^{-1}d/dt$) gives,

$$\omega_c^2 + \ddot{z}/\dot{z} - (e/m)d^2V/dz^2 = 0 \tag{7}$$

Combining Eqs. (5) and (7) we have

$$\ddot{z} + \omega_c^2 \dot{z} - \omega_p^2 M_e \dot{z}_o = 0 \tag{8}$$

where $\omega_p = \sqrt{n_o e^2/\varepsilon_o m}$, is the plasma frequency.
The solution to Eq. (8) is

$$z = \dot{z}_o \omega_c^{-1}(1 - M_e \omega_p^2/\omega_c^2)\sin \omega_c t + (M_e \omega_p^2/\omega_c^2)\dot{z}_o t$$

Define $q = \omega_p^2/\omega_c^2$ as the characteristic parameter with $q_d = M_e q$ as an effective q. Identify $a = m\dot{z}_o/eB$ as the ambient gyro-radius, and put the solution in the normalized form,

$$Z = z/a = (1 - q_d)\sin\omega_c t + q_d \omega_c t$$

with,

$$\dot{Z} = \dot{z}/\omega_c = (1 - q_d)\cos\omega_c t + q_d$$

Define a normalized potential $\Phi = V/(m\dot{z}_o^2/2e)$, and return to Eq. (6) to get

$$\Phi = (Z^2 + \dot{Z}^2 - 1) \tag{9}$$

Φ could be obtained as a function of t, but with an unnecessary increase in algebraic complexity, since we can still obtain Φ as a function of Z by obtaining Z and $\dot{Z}$ from t. Note also that

$$q = \omega_p^2/\omega_c^2 = nm/(\varepsilon_o B^2) = a^2/\lambda_D^2 \tag{10}$$

where $\lambda_D = \sqrt{\varepsilon_o kT/ne^2}$ is the Debye length.

Figure 2 shows the results of our calculation for selected values of q. The calculations were halted when $\dot{Z}$ was observed to change sign, indicating that the electron was turning around to complete its cycloid. At this point it is helpful to make a distinction between a transmitting sheath where the electron flux crosses the sheath completely, and a non-transmitting sheath where the electron flux penetrates a limited distance (and corresponding potential) and returns. The key result of our analysis is that for $q_d > 0.5$, the sheath is transmitting and the total sheath potential drop is an unlimited function of the sheath thickness. Figure 3 presents the same results as Figure 2, but with the coordinate Z, renormalized to the Debye length. From Figure 3, one can easily notice that the magnetic field does little to affect the sheath structure provided it is not so strong as to cut off the flow ($q_d < 0.5$). Figure 4, taken from Page and Adams (1958) illustrates the same result, where the current collected across a diode is little affected by B until cut off at $B > B_c$, where B_c is found from Eq. (10) by

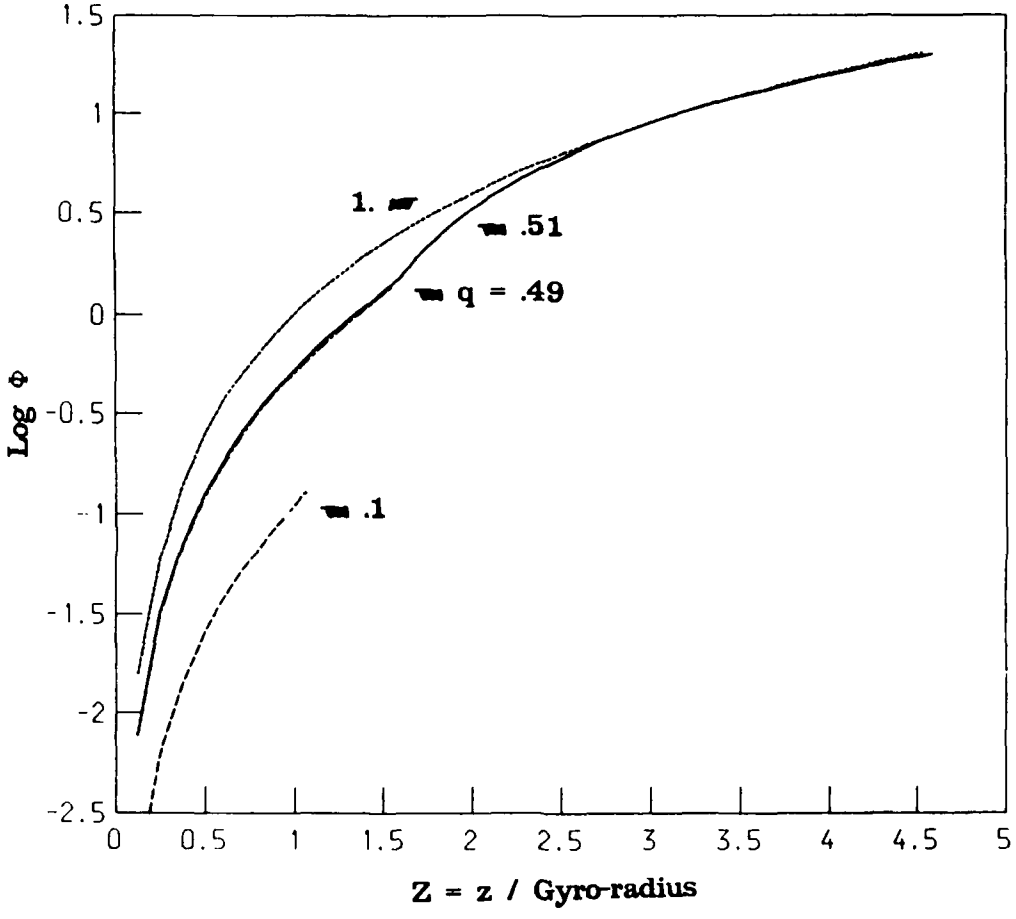

Figure 2. Plot family of the parametric solution of Φ vs sheath thickness normalized to the gyro-radius. Values of q_d are indicated on the plot. Note the termination of curves for which $q_d < 0.5$.

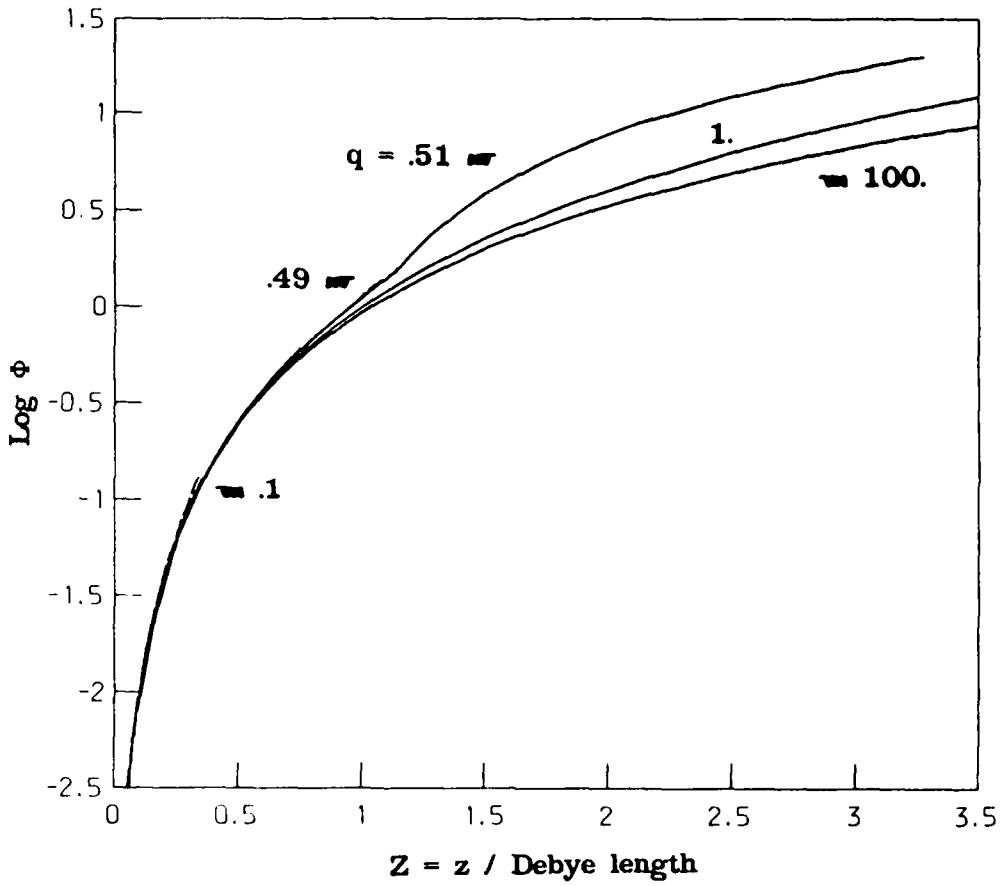

Figure 3. The same data as Figure 2 but with the sheath thickness normalized to the Debye length. Values of q_d are indicated along with the terminal points for $q_d < 0.5$.

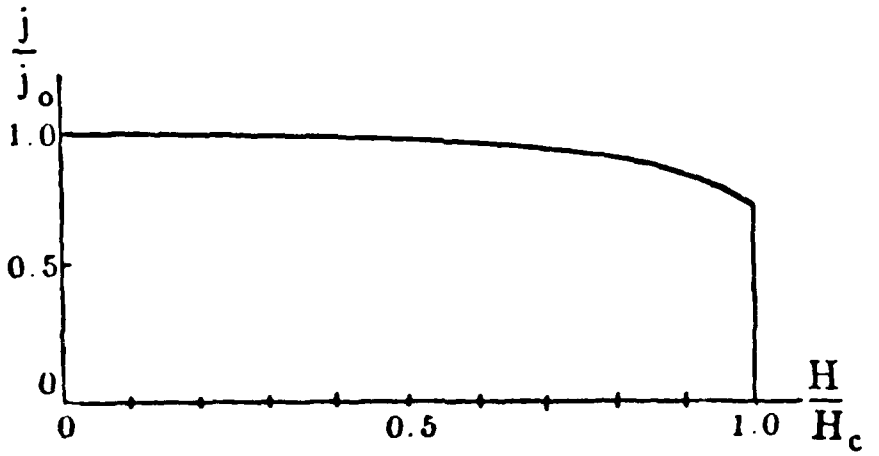

Figure 4. A plot of current vs magnetic field strength where the current is normalized to the Child-Langmuir space-charge limited current for B = 0, and B is normalized to a critical value corresponding to q = 0.5 (from Page and Adams, 1958).

setting $q_d = 0.5$. For $q_d < 0.5$ the sheath is transmitting only if the potential and thickness are less than limits obtained by setting $\dot{Z} = 0$, which gives $\omega_c t = \arccos(1-q_d^{-1})^{-1}$. For $q_d \leq 0.5$, this relation has roots of $\pi/2 < w_c t < \pi$; for $q_d > 0.5$, $\dot{Z} > 0$ always. For a given $q_d < 0.5$, the limiting $\omega_c t$ gives the limiting Φ, and Z, which are always small, i.e., $Z_{max} < \pi/2$, $\Phi < (\pi/2)^2 - 1 = 1.56$.

Consider a non-transmitting sheath with $\Phi >> \Phi_{max}$ ($q < 0.5$). For a strictly 1D problem, these conditions require an evacuated gap large enough to lower the capacitance of the gap to where the limited charge of the non-transmitting sheath equals that of the surface. This is of course a condition of magnetic insulation which can occur for some geometrical arrangements. After consideration of this possibility, and modeling in 3D with POLAR, which is discussed in the following section, we are led to the conclusion that a magnetical insulating sheath would be unlikely in any space plasma-object interactions, and that the same high B conditions that produce a non-transmitting sheath will, due to minimal increases in cycloid radii, allow charge to transport into the otherwise evacuated gap from ends any distance away. Stated otherwise, any potentially non-transmitting sheath must be considered first in three dimensions before any simplifications are attempted. It should be noted that in the low-earth-orbit ionosphere, $q > 1$ typically for ions, and $q < 1$ typically for electrons.

A possible weakness in this model is the assumption that particles enter the sheath normal to the sheath edge. Elsewhere, (Dubs & Cooke)[9] we have reworked our analysis for entry at an angle α with the x axis (sheath edge). We find that the minimum value of q for which the particles transit the sheath is $q_m = 1/(2\sin\alpha)$. Here, we have assumed $\alpha = 90°$. This model (and POLAR) should be augmented by a presheath model that accounts for the variation of α with the gyration phase of particles entering the sheath.

3. POLAR RESULTS

To test POLAR against our B-sheath model, we constructed a flat octagonal disk, pseudo radius of 3.6 meter, moving so that the plasma impinges normal to its face with B parallel to its face. The disk is at a positive potential of 43 volts, and moves at a speed of mach 8 with respect to oxygen ions, and mach 0.047 with respect to electrons. The plasma parameters are 0.2 eV temperature for ions and electrons, an ambient density of $2.0 \times 10^5/cm^3$, and a Debye length of 0.74 cm.

The POLAR method of electron tracking begins at a sheath edge, located as an equi-potential, usually 0.69 kT. External to this surface the electron distribution is presumed to be a maxwellian constrained to flow only along B. The dot product of the local sheath surface normal with B thus determines the flux and entry velocity of a super-electron which is then tracked through the sheath to determine both space-charge density and surface currents. The tracking algorithm has an efficiency motivated switch between direct integration of the Lorentz equation of motion, and guided center trajectory. The switch to guiding center tracking is made if it appears that the radius of curvature (not ambient, but the acceleration affected curvature) will be less than the dimensions of the upcoming volume element. We demonstrate that this causes a grid dependence of the results when the resolution

---

9. Dubs, C.W. and Cooke, D.L. (1987) *Particle Trajectories and Potentials in a Plane Sheath Moving in a Magnetoplasma*, AFGL-TR-87-0225, AD A196228

is too coarse, but with sufficiently fine gridding, gives remarkably good agreement with our B-sheath predictions.

Model 1 is a POLAR-disk model with B = 0.2 Gauss, q = 56, and q_d = 2.6. Figure 5 presents 2-D cut in the plane of the flow vector (+Z, from the left) and B (+Y, out of the page, thus, along the leading face) any E x B drift will be +X. Figure 5 shows the equi- potential contours, while Figure 6 shows the sheath surfaces and particle tracks with the contours removed for clarity. A wake structure characterized by weak negative potentials can be observed in the figures. Note that the electron emitting sheath edge (– symbol) is smooth, and most of the electron tracks traverse the sheath to the face. This is the anticipated behavior as both q and q_d are greater than 0.5. Figure 7 shows the POLAR solution for B = 0, which can be seen to be qualitatively similar to model 1.

For model 2, Figure 8, B is increased to 0.3 Gauss with q = 22.0, and q_d = 1.1. The sheath still has the nominal no-B appearance, but many electrons are starting to drift along the sheath edge.

In model 3, Figure 9, B is increased to 0.5 Gauss, with q = 8.2 and q_d = 0.38. Radically different electron behavior is observed, with most ram electrons drifting parallel to the sheath edge, giving rise to strong spatial perturbations of the sheath edge. It should be noticed that there is still significant space charge in the sheath, but that it is now coming from the edges of the disk.

Figure 10 is a replay of model 1, but with the grid resolution reduced by half. The tendency towards premature guiding center treatment can be observed in the increased number of drifting trajectories as if q_d had been reduced. In this case, the ram side sheath is resolved with about three mesh intervals, which would be the limit of POLAR's accuracy with or without a magnetic field due to the non-linear nature of a sheath.

4. DISCUSSION AND CONCLUSIONS

Linson[10] has previously observed the importance of q in determining electron sheath physics, and the tendency for crossed field (E and B) beams to be unstable for q ~ 0.5. POLAR is not a time dependent simulation code, but the standing waves on the surface of our lowest q sheath might be construed to be an artifactual analog of the electrostatic instability invoked by Linson and studied by Bunemann and Linson[11]. Our study of the B-sheath leads us to disagree with Linson on the point that for q > 0.5, turbulence is not needed for the transport of electrons across B. However, instabilities at the sheath edge may still play an important role in increasing the electron flux through the sheath edge and narrow the gap between the plasma q and the effective q_d for the sheath.

We may now also tie together our previous conclusion about the inescapability of end effects for the long 'cylinder' problem, and the problem that arises with q_d when an object is stationary, and the ambient gyro radius is small compared to the cylinder radius. In this case, electrons find their way to the sheath edge only along B, so there will be no flux through the sheath if its edge is exactly parallel to B. This is no problem if B is so strong (q_d < 1) that charge transporting along B within the sheath (from

---

10 Linson, R.H. (1969) Current-voltage characteristics of an electron-emitting satellite in the ionosphere, *J. Geophys. Res.* **74**:9.

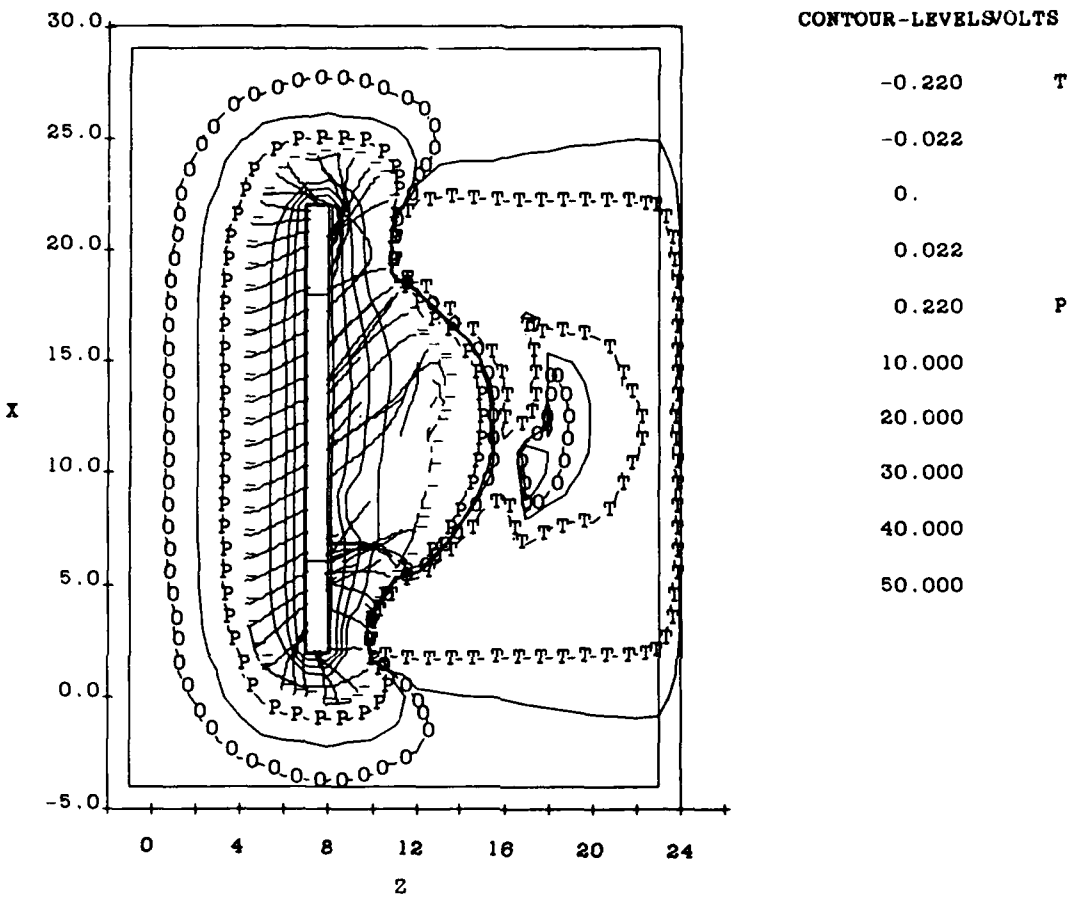

MODEL 1 $q = 51.4$, $q_d = 2.6$, $B = 0.2$ G ⊙

$M_i = 8.0$, $M_e = 0.05$, $V_o = 43.0$ v , $R = 1.8$ m

$N_o = 2.0 \times 10^5$ cc^{-1} , $kT = 0.2$ eV, $\lambda_d = 0.74$ cm

Figure 5. POLAR 2D slice plot through the middle of the 3D grid and disk. Plasma flows from the left. Electron trajectories are started (symbol -) just inside the sheath edge (symbol P). The zero potential contour is indicated by a 0, and T marks the negative potential sheath edge where ion trajectories could be, but were not initiated. Coordinate scale is in grid units of 0.18 meters.

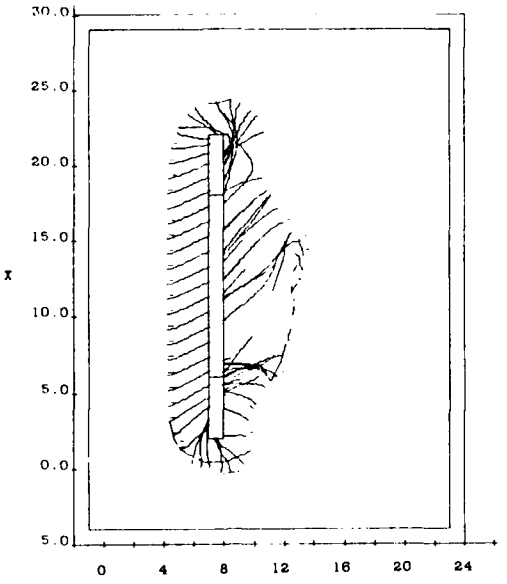

Figure 6. Model 1 with just electron trajectories.

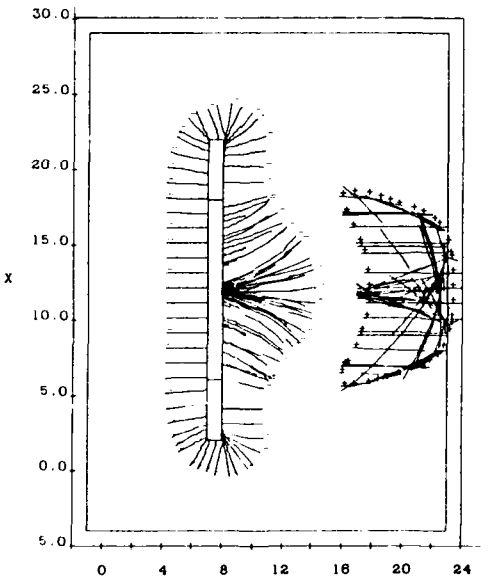

Figure 7. Similar model, but with $B = 0$, $q = \infty$.

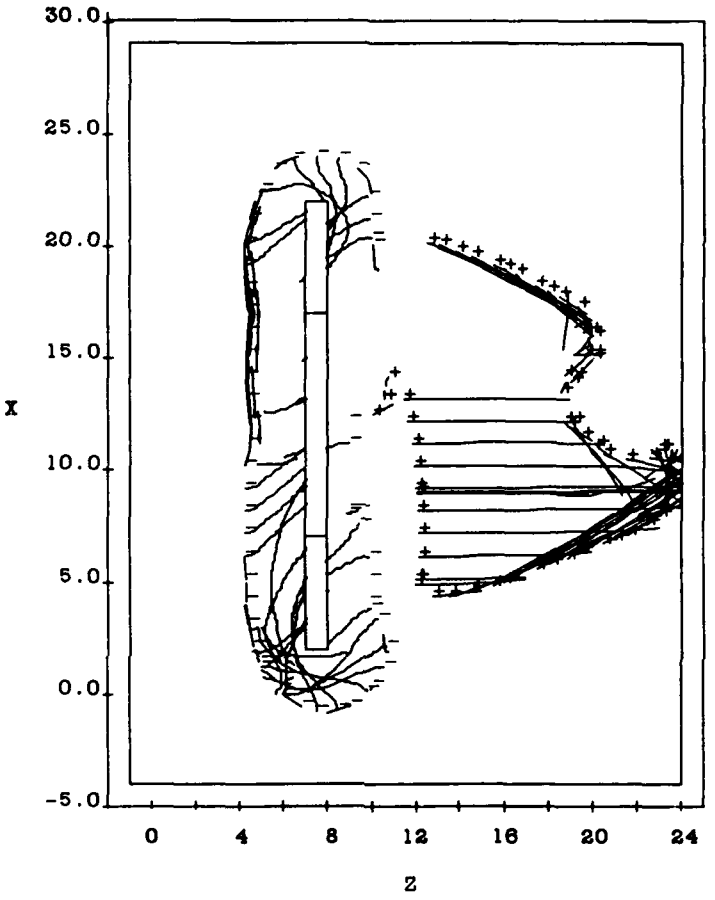

MODEL 2 $q = 22.0$, $q_d = 1.1$, $B = 0.3$ G ⊙

$M_i = 8.0$, $M_e = 0.05$, $V_o = 43.0$ v , $R = 1.8$ m

$N_o = 2.0 \times 10^5$ cc^{-1} , kT = 0.2 eV, $\lambda_d = 0.74$ cm

Figure 8. POLAR 2D slice plot through the middle of the 3D grid and disk. Plasma flows from the left. Electron trajectories are started (symbol -) just inside the sheath edge. The symbol + marks where the ions are started inside the negative potential sheath edge. Coordinate scale is in grid units of 0.18 meters.

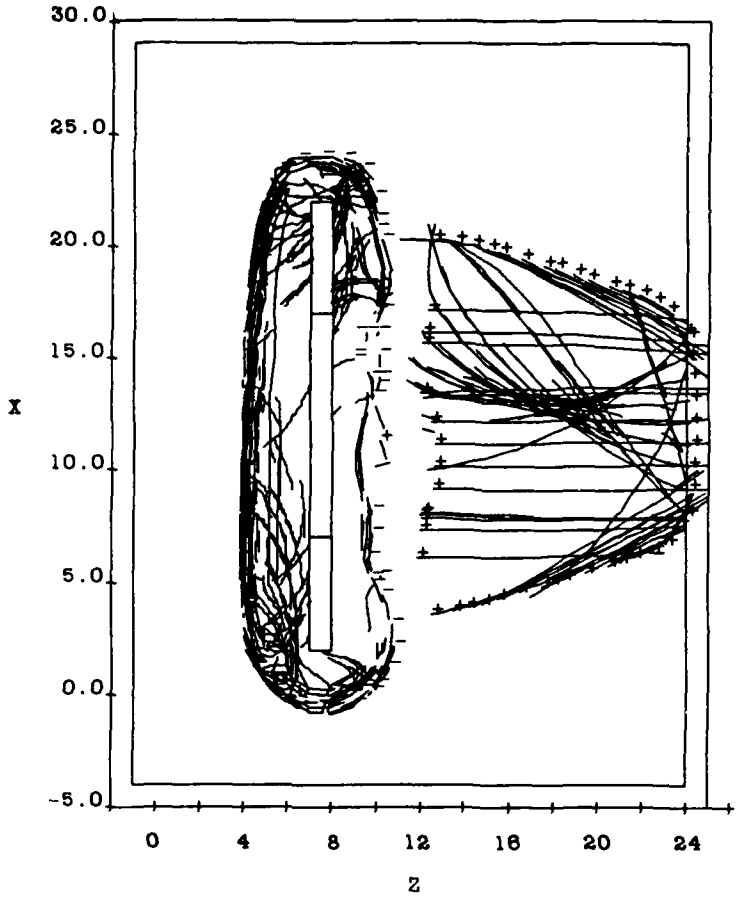

MODEL 3 $q = 8.2$, $q_d = 0.4$, $B = 0.5$ G ⊙

$M_i = 8.0$, $M_e = 0.05$, $V_o = 43.0$ v , $R = 1.8$ m

$N_o = 2.0 \times 10^5$ cc^{-1} , $kT = 0.2$ eV, $\lambda_d = 0.74$ cm

Figure 9. POLAR 2D slice plot through the middle of the 3D grid and disk. Plasma flows from the left. Electron trajectories are started (symbol -) just inside the sheath edge. The symbol + marks where ions are started inside the negative potential sheath edge. Coordinate scale is in grid units of 0.18 meters.

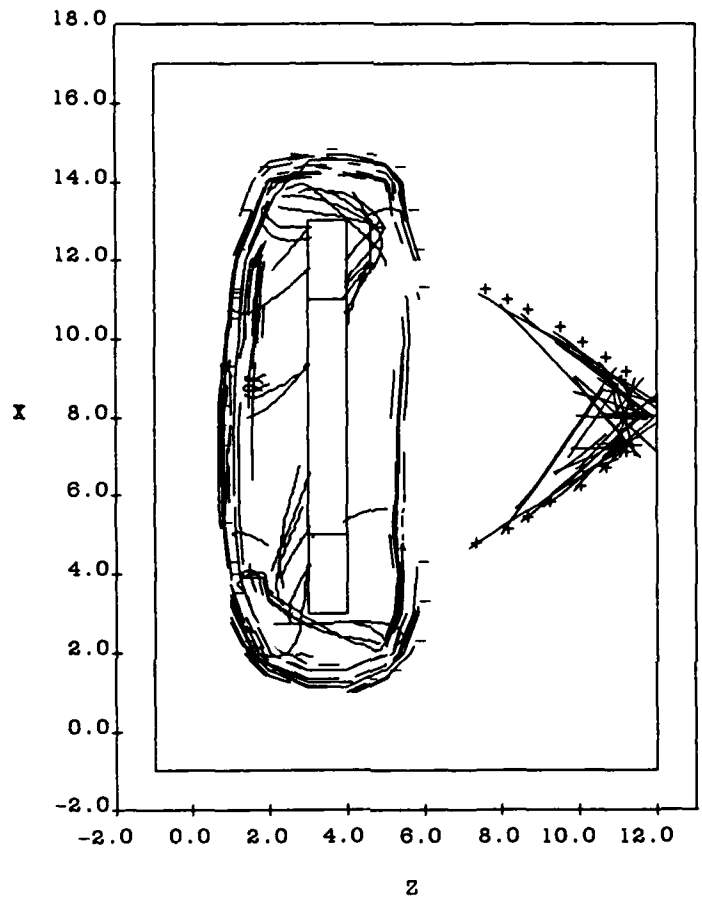

MODEL 1 Grid Test ; $q = 56.0$, $q_d = 2.6$, $B = 0.1$ G ⊙

$M_i = 8.0$, $M_e = 0.05$, $V_o = 43.0$ v , $R = 1.8$ m

$N_o = 2.0 \times 10^5$ cc^{-1} , kT = 0.2 eV, $\lambda_d = 0.74$ cm

Figure 10. Rerun of Model 1, but with Grid Resolution Halved to 0.36 Meter/Grid Unit.

the ends) provides charge for the shielding. For $q \leq 0.5$, however, this end-effect charge will still undergo an enlargement of the individual cycloids, causing some of this charge to impact the cylinder surface. This would lead to an enlargement of the sheath and a sheath edge making an angle with B, thus allowing a flux to the sheath edge and a non-zero q_d.

We conclude by commenting on the value of modeling. In this study, our end effect conclusion was greatly influenced by its unavoidable presence in the POLAR models.

References

1. Cooke, D.L., Katz I., Mandell, M.J., Lilley, J.R., Jr., and Rubin, A.J. (1983) Three-dimensional calculation of shuttle charging in polar orbit, in proc. *Spacecraft Environmental Interactions Tech.* Conf. ed. by C.K. Purvis and C.P. Pike, NASA Conf. Pub. 2359, AFGL-TR-85-0018.
2. Lilley, J.R.,Jr., Cooke, D.L., Jongward, G.A., and Katz, I. (1985) *Polar User's Manual*, AFGL-TR-85-0246, AD A173 758.
3. Rubinstein, J. and Laframboise, J.G. (1983) Theory of axially symetric probes in a collisionless magnetoplasma: aligned spheroids, finite cylinders, and disks, *Phys. Fluids* **26**:12.
4. Parker, L.W. and Murphy, B.L. (1967) Potential buildup on an electron-emitting ionospheric satellite, *J. Geophys. Res.* **72**:5.
5. Page, L. and Adams, N.I., Jr. (1946) Space charge in plane magnetron, *Phys. Rev.* **69**:9, 10.
6. Birdsall, C.K. and Bridges, W.B. (1966) *Electron Dynamics of Diode Regions*, Academic Press Electrical Science Series.
7. Child, C.D. (1911) Discharge from hot CaO, *Phys. Rev.* Ser. I, **32**:492.
8. Langmuir, I. (1923) The effect of space charge and initial velocities on the potential distribution and thermionic current between plane parallel electrodes, *Phys. Rev.* **21**:419.
9. Dubs, C.W. and Cooke, D.L. (1987) *Particle Trajectories and Potentials in a Plane Sheath Moving in a Magnetoplasma*, AFGL-TR-87-0225, AD A196228.
10. Linson, R.H. (1969) Current-voltage characteristics of an electron-emitting satellite in the ionosphere, *J. Geophys. Res.* **74**:9.
11. Bunemann, O., Levy, R.H. ,and Linson, R.H. (1966) Stability of crossed-field electron beams, *J. Ap. Phys.* **37**:8, 3203.